Hindawi
Advances in Materials Science and Engineering
Volume 2021, Article ID 2588784, 12 pages
https://doi.org/10.1155/2021/2588784

Research Article

Lubrication Effect of Polyvinyl Alcohol/Polyethylene Glycol Gel for Artificial Joints

Shoujing Zhang,[1] Feng Hu,[1] Jianhui Li,[2] Leifeng Lv,[3] and Hailin Lu[1]

[1]*Group of Mechanical and Biomedical Engineering, Xi'an Key Laboratory of Modern Intelligent Textile Equipment, College of Mechanical & Electronic Engineering, Xi'an Polytechnic University, Xi'an, Shaanxi 710048, China*
[2]*Nanotechnology Center, Institute of Textiles & Clothing, The Hong Kong Polytechnic University, Hung Hom, Kowloon, Hong Kong 999077, China*
[3]*Department of Orthopedics, The Second Affiliated Hospital of Xi'an Jiaotong University, Xi'an Jiaotong University, Xi'an, Shaanxi 710061, China*

Correspondence should be addressed to Jianhui Li; jianhui.li@polyu.edu.hk, Leifeng Lv; 15529351957@163.com, and Hailin Lu; lu@xpu.edu.cn

Received 6 May 2021; Revised 3 July 2021; Accepted 26 July 2021; Published 2 August 2021

Academic Editor: Tomasz Trzepieciński

One of the most common problems encountered by patients using artificial joints is the high wear rate. In this study, a polyvinyl alcohol/polyethylene glycol (PVA/PEG) gel was prepared through the cross-linking reaction between polyvinyl alcohol (PVA) and polyethylene glycol (PEG) solutions. This gel can lubricate artificial joints, thereby lowering their coefficient of friction (COF) and increasing their service life. Various techniques, such as Fourier transform infrared spectroscopy, X-ray diffraction, Raman spectra, X-ray photon spectroscopy, and thermogravimetric analyses, were used to analyze the structure of this synthetic gel. The tribological results indicated that the synthetic gel's lubrication effect was the most optimum when it contained PVA (10 wt%) and PEG (15 wt%). An average COF of 0.05 was obtained under a load of 10 N and at a speed of 1.0 cm/s. In addition, the wear rate was reduced in comparison to distilled water. Furthermore, the biological tests proved that the PVA/PEG gel was highly biocompatible. Thus, this study introduces a novel technique to prepare PVA/PEG gels that improve the tribological performance of artificial joints.

1. Introduction

The applications of gels have rapidly increased and become diversified. Gels can repair soft tissues, fill tissue cavities, and address other soft tissue defects [1–4]. Patients suffering from different joint diseases can opt for joint replacements [5, 6]. However, frictional and general wear reduce the service life of artificial joints [7–9]. Several different solutions have been proposed to mitigate this problem [10, 11]. Polyether ether ketone (PEEK) is a biomaterial that is used to create artificial joints for joint replacement [12, 13] and is widely used by researchers in other research in the field of prosthetic implants [14–17]. Several materials are used to prepare artificial joints, and one such material is CoCrMo alloy [18–21].

The coefficient of friction (COF) of the natural joints in the human body ranges from 0.001 to 0.03 under a pressure range of 3–18 MPa, which is lower than that of most artificial joints [22]. However, the lubrication of artificial joints is not easy because the lubricants should be easily absorbed by the human body. In addition, fragments of materials produced during friction could lead to inflammation [23–25]. Therefore, the development of alternative lubrication methods to increase the service life of artificial joints has attracted considerable attention [26–29].

Polymers are high-molecular-weight compounds that are repeatedly linked by covalent bonds. The reaction between different macromolecules is called cross-linking reaction [30, 31]. Katta et al. reported that polyvinyl alcohol/polyvinylpyrrolidone (PVA/PVP) was cross-linked into

hydrogels and investigated for its potential use as cartilage replacement [32]. Li et al. prepared chemical-physical cross-linked trimesh (TN) hydrogels using PVA, PVP, and acrylic acid as raw materials. The effects of Zn^{2+} on the mechanical and frictional properties of hydrogel were studied by controlling the content of Zn^{2+} in TN hydrogel [33]. Polyvinyl alcohol (PVA) gel is biocompatible and can act as a lubricant, but its high melting point limits its applicability [34–36]. Copolymerization or macromolecule reactions can be used to introduce weak forces into the main chain or side group of the molecule. This weakens the intramolecular and intermolecular forces of the PVA molecule, thereby reducing the melting point [37]. Polyethylene glycol (PEG) is widely used for lubrication purposes and is biodegradable and biocompatible [38, 39]. Therefore, in this study, PEG was added to PVA to form a composite gel for artificial joint lubrication using a novel gel preparation technique.

It is important for the prepared gel to be biocompatible, biodegradable, and nontoxic for clinical applications [40]. PVA solution was added to a PEG solution to obtain a PVA/PEG gel in this study. Both PEG and PVA contain a large number of hydrogen-containing functional groups on their surfaces; therefore, when PEG is added to PVA, a large number of hydrogen-containing functional groups are bound together by hydrogen bonding [41–43]. Gel lubrication is preferable to liquid lubrication for clinical applications because the gel forms a membrane, preventing direct contact between joints. This PVA/PEG gel improves lubrication between artificial joints and thus extends their service life.

2. Experimental Method

2.1. Materials. PEG (molecular weight: 4,000 Da) and PVA were purchased from Tianjin Damao Chemical Reagent Factory. The materials used in this study were of analytic reagent (AR) grade.

2.2. Preparation of Samples. Different PEG weights were added to different amounts of distilled water to obtain PEG solutions with varying concentrations (10, 15, 20, and 25 wt %). PVA (10 g) was added to 90 mL of distilled water, heated at 90°C, and stirred at 500 rpm for 20 min to obtain a 10 wt% PVA solution; subsequently, the temperature was maintained at 70°C. The PVA solution (20 mL) was then added to the PEG solution (50 mL). Following that, the solutions were mixed by magnetically stirring the mixture at 70°C and 500 rpm for 20 min to obtain the PVA/PEG gel. This process was repeated for different PEG solution concentrations under identical conditions to obtain gels with varying concentrations. The PVA/PEG gels were then stored in a room at 25°C for 24 hours.

2.3. Friction Tests. The tribological properties were investigated using the GSR-2 friction machine (rubber alcohol friction testing machine, China). The samples were made to slide against a disk with a reciprocation friction drive system at room temperature (25°C). The disk was made of CoCrMo alloy plates (Φ 30 mm). A PEEK ball (Φ 9.525 mm) was made to slide against the disk. A 3–10 N load was applied for 30 min. The specifications of the materials, as provided by the manufacturer, are listed in Table 1. The tests were repeated three times, and the average values of these results were used for analysis.

2.4. Characterization. Fourier transform infrared (FT-IR) spectroscopy was used to study specific interactions. The samples were scanned for waves with wavelength numbers between 500 cm^{-1} and 4,000 cm^{-1} using the Nicolet iS50 spectrometer (Thermo Fisher Scientific, USA). The crystal phase structure patterns were analyzed through X-ray diffraction (XRD) characterization using the D8 ADVANCE diffractometer (Bruker, Germany). Raman spectra of the two materials were obtained using Horiba Jobin Yvon, Model Hr800, under the following conditions: laser wavelength 514 nm, output 17 mW, grating 600, objective ×10, time 10 s, and wavenumber 500–4,000 cm^{-1}. X-ray photoelectron spectroscopy (XPS) was performed using the ESCALAB 250Xi X-ray photoelectron spectrometer (Thermo Fisher Scientific, USA) to study the elemental composition of the material. The gels were dried at 37°C for 24 hours in a vacuum oven. Thermogravimetric analyses (TGA) were performed using the 409C thermobalance (NETZSCH Group, Germany) at temperatures ranging from 25°C to 920°C in an oxygenated atmosphere.

2.5. Biological Tests. The three materials (PEG, PVA, and PVA/PEG) were placed in appropriate amount of PBS, and the gel solution with a mass volume fraction of 100 mg/mL was obtained through applying high temperature and high pressure. The cell complete medium components were 10% fetal bovine serum (Gibco), 100 U/mL penicillin, and 100 μg/mL streptomycin (Gibco) and RPMI1640 (Gibco). Third-generation resuscitated L929 cells were used for the experiment. After the cells grew to about 80%, the medium was discarded and washed twice with sterile PBS, and trypsin (GBICO) was added for digestion for a duration of 1 min. Digestion was stopped with the complete medium, resuspended, and centrifuged. The supernatant was discarded, and the complete medium was added to the cell precipitates to obtain the cell suspension again. The cell suspensions were mixed and counted. The cell density was 10,000 cells per well, and the total amount of medium in each well was 150 μL. The cell is cultured at 37°C in a 5% CO2 incubator for 12 hours. Subsequently, 10 μL of PEG, PVA, or a mixture of PEG and PVA was added to each well, and the wells were divided into four groups: PEG, PVA, PEG/PVA, and blank control groups. Each group had six duplicate holes. The culture was incubated at 37°C in 5% CO_2. After 24 h, the material and medium were discarded; sterile PBS was gently washed twice, and the complete medium containing 10 μL CCK8 solution was added to each well for further incubation for 1 h. The solution was fully mixed by shaking at a low speed for 10 min on a shaking table. FLUOstar Omega analyzer was used to detect the OD value of each hole at 450 nm.

Table 1: The performance of tests materials.

Materials	Yield strength (MPa)	Young's modulus (GPa)	Tensile strength (MPa)	Density ($g \times cm^{-3}$)
PEEK	110	0.305	527	1.5
CoCrMo	310	210	860	8.3

3. Results and Discussion

3.1. FT-IR, XRD, and Raman Analysis. Figure 1(a) shows the FT-IR spectra of the PVA, PEG, and PVA/PEG gels. The absorption peaks of the FT-IR plot of PVA at 1,087 cm^{-1} and 2,886 cm^{-1} can be attributed to the asymmetric vibration of C–O–C and O–H vibration, respectively [44]. The absorption peak of the PEG FT-IR plot at 1,096 cm^{-1} is similar to that of PVA, indicating that a C–O–C asymmetric vibration could be responsible for the PEG peak as well. The absorption peak at 2,883 cm^{-1} was attributed to the stretching modes of CH_2 in PEG [45, 46]. The wideband around 3,349 cm^{-1} is thought to be due to the stretching vibrations of the hydroxyl group [47]. Figure 1(b) shows an enlarged FT-IR plot of the PVA/PEG gel. Although the plot of the gel contained two absorption peaks at 2,884 cm^{-1} and 1,144 cm^{-1}, as shown in the magnified plot in Figure 1(b), they were insignificant in comparison to the raw material. This could be due to the lower substance content. This indicates that the tensile vibration of the two materials in the PVA/PEG gel, which is attributed to the interaction between PVA and PEG, led to a redshift. Figure 1(c) shows the XRD patterns of PVA, PEG, and the PVA/PEG gel. The PVA/PEG gel had two diffraction peaks at 19.1° and 23.1°, which are similar to the characteristic peaks of PEG. However, the diffraction peaks of PEG have relatively large intensities and widths and are greater than 19.1° and 23.1°. The characteristic peak at 19.5° corresponds to PVA. This indicates that the crystallinity of PVA/PEG is lower than that of pure PEG, thereby proving that the interactions between PVA and PEG in the gel affect the crystallinity of PEG. Figure 1(d) shows the Raman spectra of 10 wt% PVA and PVA/PEG (10 wt %/15 wt%) gels. PVA has evident characteristic peaks at 856 cm^{-1}, 919 cm^{-1}, 1,446 cm^{-1}, and 2,916 cm^{-1}. The characteristic peaks of PVA/PEG are similar to those of PVA but with higher intensity. This indicates that the special structure formed after the interaction between PVA and PEG leads to peak enhancement.

3.2. XPS and TGA Analysis. The composition and chemical states of the elements were analyzed using an X-ray photoelectric spectrometer. The XPS spectral peak of O 1s is observed at 532 eV, as shown in Figure 2(a). This can be attributed to the presence of the O–H bonds [48]. The Gaussian distribution contains three peaks at 284.3 eV, 285.9 eV, and 288.7 eV, as shown in Figure 2(b). The different peaks are attributed to the presence of C bonds in ethylene and carbon and carbonyl carbon in CH_2 [49]. The 284.3 eV and 532 eV peaks correspond to the O and C elements in PVA/PEG, respectively, as shown in Figure 2(c). The mass of these two materials reduces with increase in temperature. The thermal decomposition rate of the PVA/PEG gel was relatively low below 252°C, as shown in Figure 2(d). This is attributed to the interactions between PVA and PEG and a rise in the crystallinity of the polymer. The thermal decomposition rate of PVA is greater than that of the PVA/PEG gel at a given temperature beyond 252°C because of the presence of PEG in the PVA/PEG gel.

3.3. The Lubrication Effect of Different Materials. Different materials produce different lubrication effects. The conditions were fixed at 2.0 cm^{-1} and 10 N in this section. Figure 3(a) shows the transient variation of the COF of five materials. Water lubrication produced a relatively high COF that gradually increased with time because of the rise in the contact area. PVA/PEG gels with different concentrations were obtained by adding different concentrations of PEG solution to 10 wt% PVA. It can be seen that the overall COF increases with time; however, the PVA/PEG gel at 15 wt% PEG concentration has the best lubrication effect, and the overall COF is the lowest. Figure 3(b) shows the average COF of various materials within 30 min. The PVA/PEG gel (10 wt%/15 wt%) exhibited the lowest COF among the tested materials. The average COF of the gel (10 wt%/15 wt%) was 0.11, which was approximately two-thirds of that of water (0.15); it was also lower than that of the other gels, indicating that this gel was most effective in reducing friction.

3.4. The Lubrication Effect of Different Loads. The previous section demonstrated that the PVA/PEG gel with a concentration of 10 wt% and 15 wt% was more effective than the other gels. However, the gel may be subjected to different pressures in different human bodies. A single load trial is insufficient to analyze an artificial joint. Therefore, we tested the COF for different loads, as shown in Figure 4(a), which demonstrates that the effect of friction increased with an increase in load and displayed a relatively stable trend. This is because the increased load squeezes out the PEG molecules in the gel, thereby releasing more lubricant in a short duration [50]. It is evident from Figure 4(b) that the average COF under 10 N is lower than that under different loads. This also verifies that the lubricating material can be effectively extruded under higher loads. In addition, the average pressure of the contact surface under different pressures is calculated according to the Hertz contact theory [51, 52]. It can be seen that the average contact pressure increases with the increase in load. However, the gel exhibits better lubrication at higher pressures. Thus, these data indicate that the lubrication effect of these gels improved with increasing pressure.

3.5. The Lubrication Effect at Different Speeds. Figure 5(a) shows the effect of the sliding speed on the COF. The final

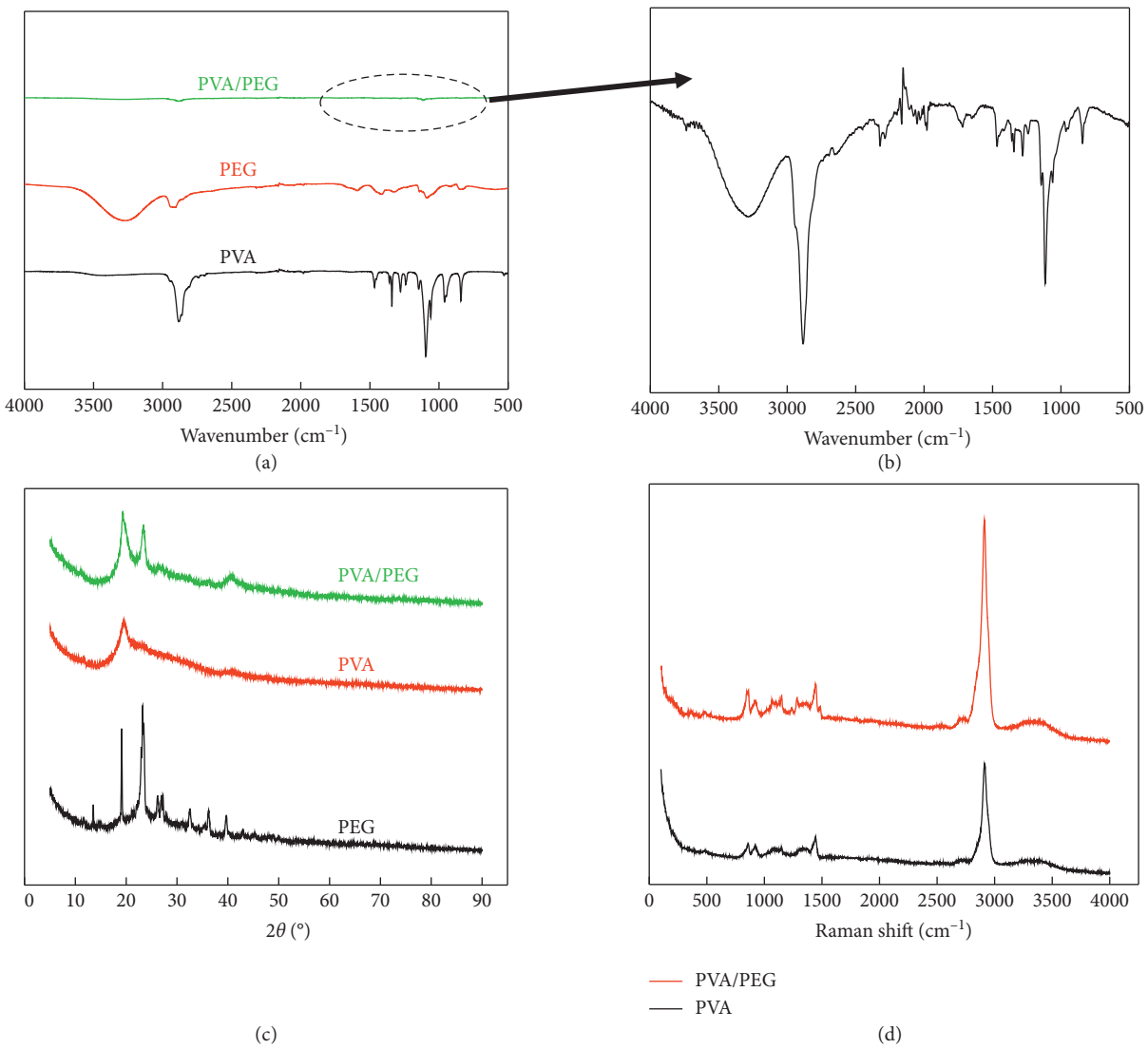

Figure 1: (a) FT-IR spectra; (b) enlarged view of the FT-IR spectra; (c) XRD patterns of PEG, PVA (10 wt%), and PVA/PEG (10 wt%/15 wt %); and (d) Raman spectra of PVA (10 wt%) and PVA/PEG (10 wt%/15 wt%).

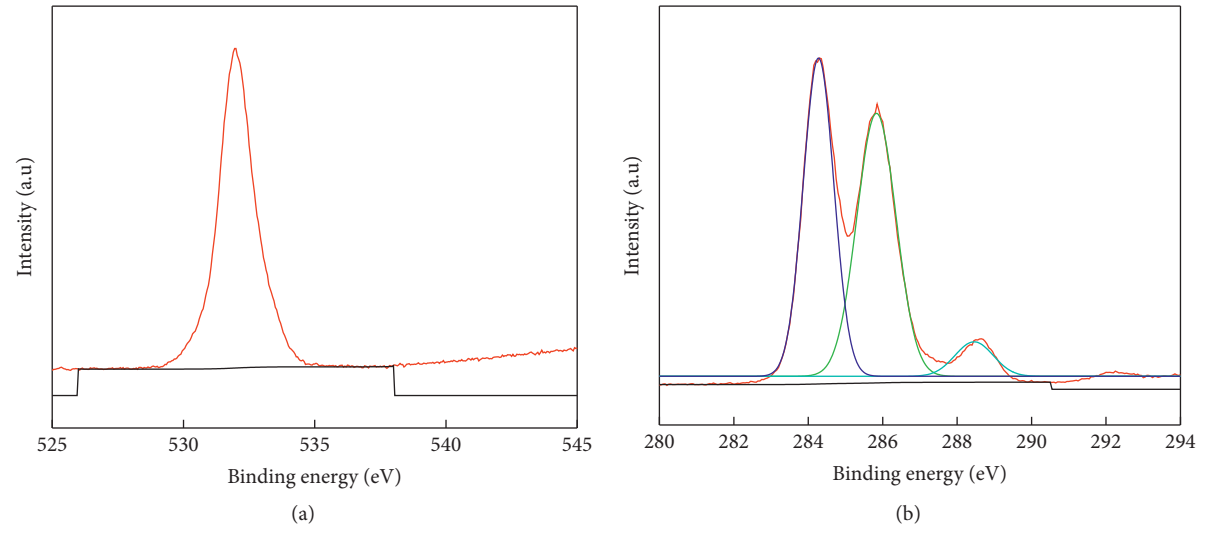

Figure 2: Continued.

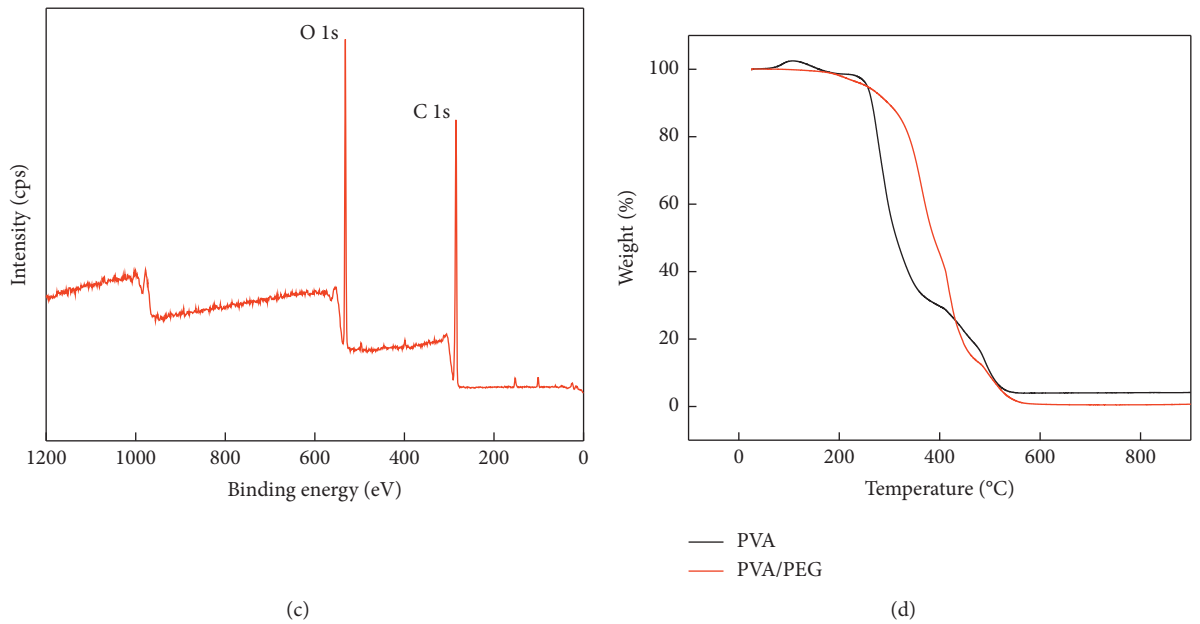

Figure 2: (a) O 1s XPS spectra of PVA/PEG, (b) C 1s XPS spectra of PVA/PEG, (c) XPS spectrum of PVA/PEG (10 wt%/15 wt%), and (d) TGA curves.

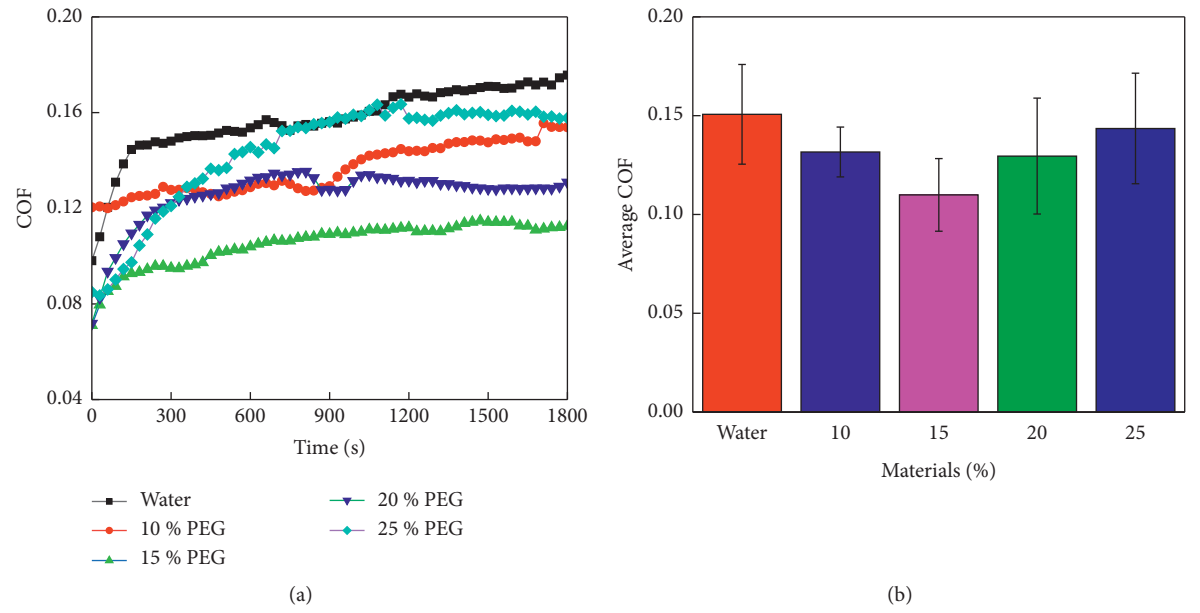

Figure 3: (a) COF curves and (b) comparison of the COF values of distilled water and PVA/PEG gels with different concentrations.

COF increases with time for all speeds. The overall COF was relatively large for a wavenumber of 2.0 cm^{-1}. The variation of the average COF with speed is illustrated in Figure 5(b). The gel lubrication and COF were maximum and minimum, respectively, at a sliding velocity of 1.0 cm/s for the PVA/PEG gel (10 wt%/15 wt%). Most solid materials follow Amontons' law of friction [53], which states that the COF depends only on the positive load. The results shown in Figure 5 indicate that the PVA/PEG gel does not follow this model because the COF depends on the normal load as well as on the sliding speed. The COF of the PVA/PEG gel increased within a certain range when the sliding velocity was greater than 1 cm/s. This can be attributed to the insufficient release of lubricating substances at high speeds, which inhibits lubrication.

3.6. Influence of Moisture Content on Lubrication Effect. The gel was soaked in water for certain duration after it had been dried to test the influence of the moisture content of the

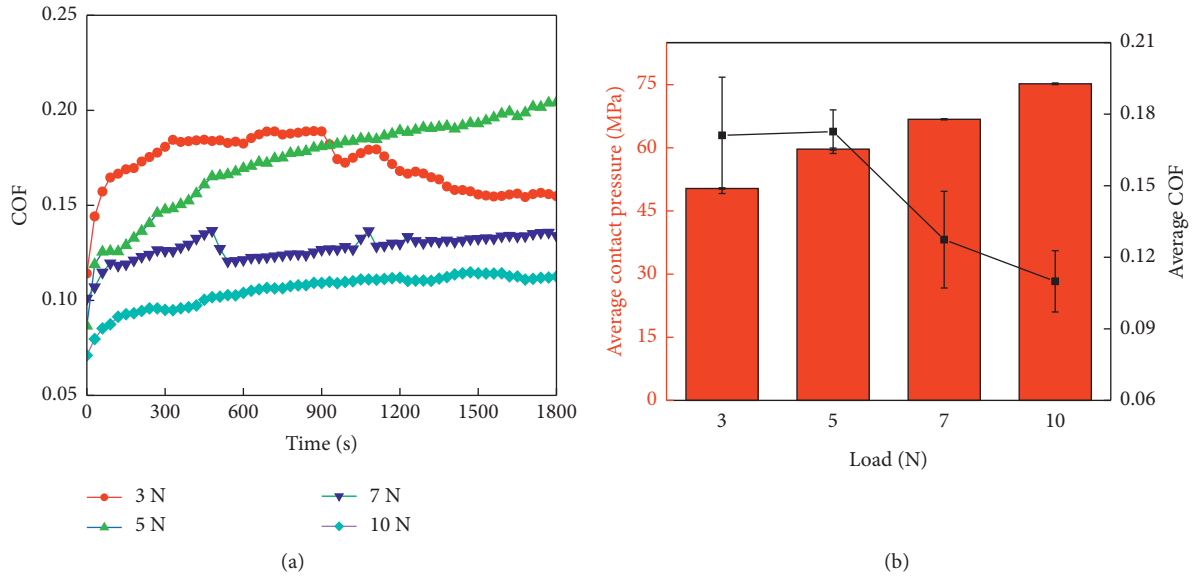

Figure 4: (a) Transient variation of COF for different loads and (b) variation of the average COF with a load.

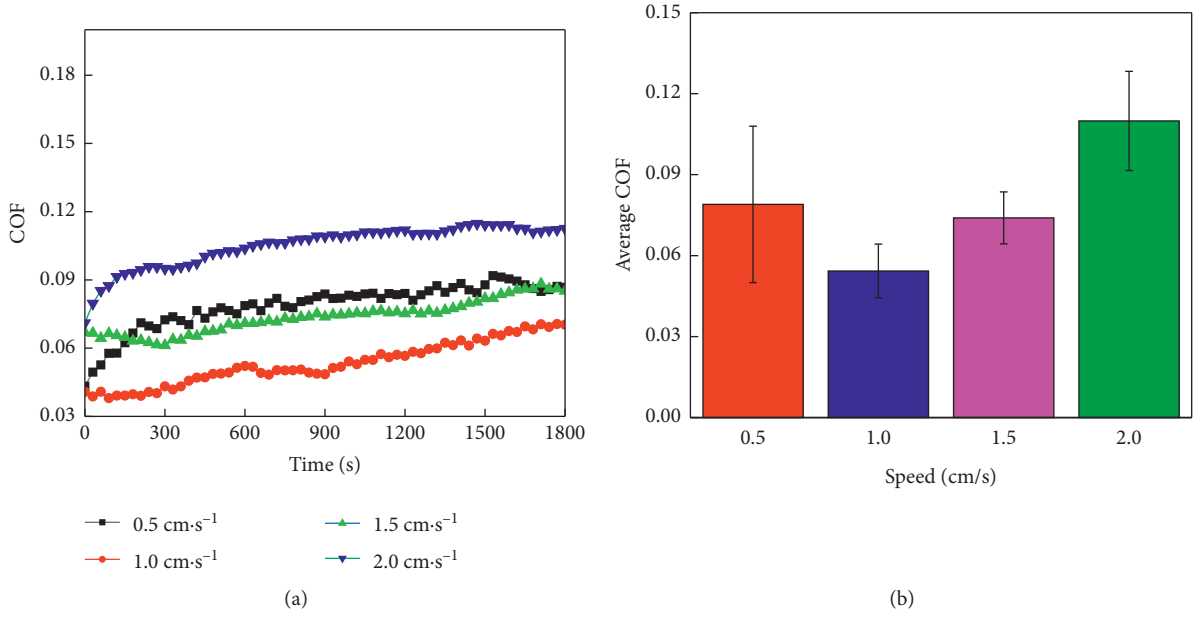

Figure 5: (a) Transient variation of COF for different speeds and (b) variation of the average COF with speed.

gel on lubrication. As seen from Figure 6(a), the COF decreases as the number of days for which the gel was soaked increases because the lubricating substances in the gel are not easily released after drying. This is attributed to the reduction in the COF after soaking. The average COF of the 10 wt% PVA/15 wt% PEG gel decreases as shown in Figure 6(b). These results demonstrate that the gel can be reimmersed after dehydration to restore its original lubrication capacity, which presents a feasible solution for large-scale use or production at later stages.

3.7. Wear Analysis of CoCrMo Alloy Disk. Figure 7 shows four CoCrMo alloy disks under an optical microscope. Figure 7(a) shows an image of a water-lubricated worn surface. There are obvious scratches on the disk, which form a wideband due to the inability of water to reduce wear. An image of a disk subjected to 10 wt% PVA as a lubricant is shown in Figure 7(b). The wear range is improved in comparison to that of distilled water; however, this improvement is insignificant. Figure 7(c) shows the image of a CoCrMo subjected to 15 wt% PEG as a lubricant. Although the material demonstrated a low COF in the tests, the wear images indicated a high rate of wear and the presence of marked stripe scratches. Figure 7(d) shows an image of the disk subjected to PVA/PEG gel (10 wt%/15 wt%) as a lubricant. The wear rate is significantly lower than that of the other lubricants. In addition, the COF for this gel is less than

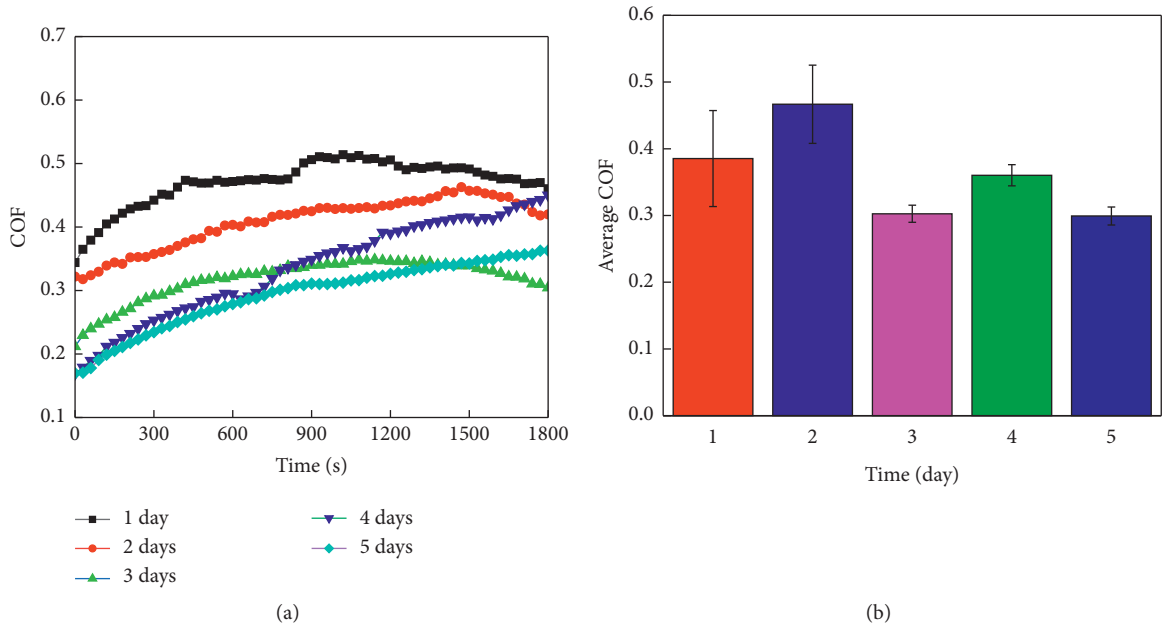

Figure 6: (a) Transient variation of COF on different days and (b) variation of the average COF with the number of days.

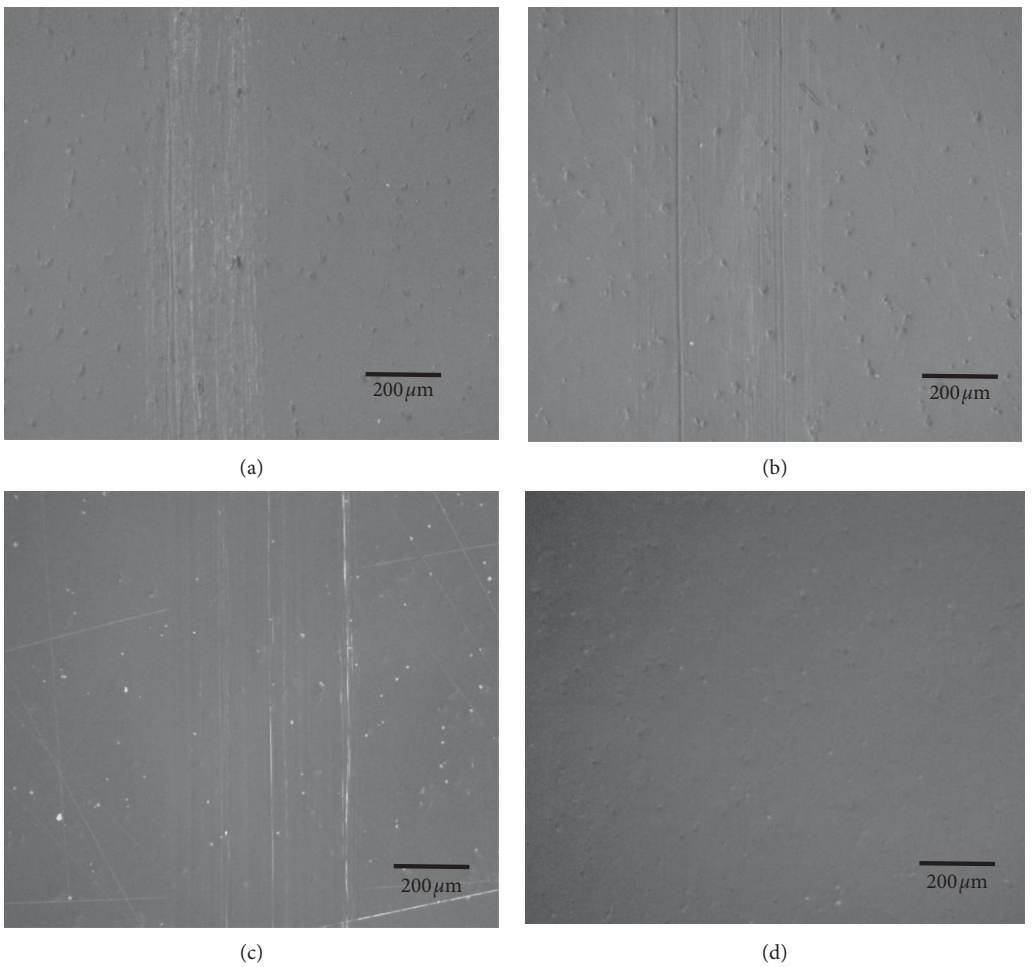

Figure 7: Surfaces of the CoCrMo alloy disks subjected to different lubricants, such as: (a) water, (b) PVA, (c) PEG, and (d) PVA/PEG gel.

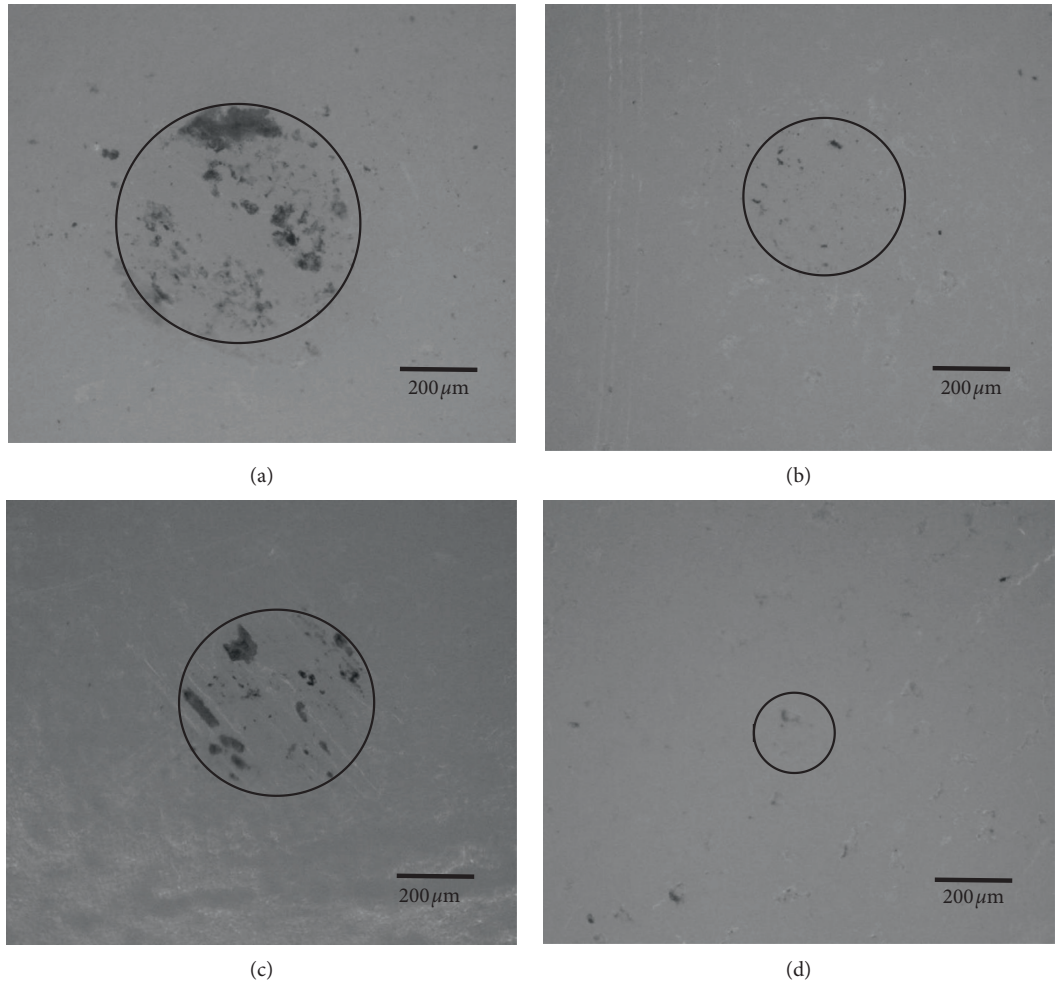

Figure 8: Worn surface of the PEEK ball subjected to different lubricants, such as: (a) water, (b) PVA, (c) PEG, and (d) PVA/PEG gel.

that of the other lubricants. This is because the gel utilizes the positive effects of both its components. The film formed by the gel during wear is reduced, and the lubrication effect is enhanced because of the influence of PEG.

3.8. Wear Analysis of PEEK Ball. Figure 8 shows four microscopic images of PEEK balls subjected to different lubricants. Figure 8(a) shows an image of a water-lubricated worn surface of a PEEK ball. The large wear volume is evident in the image; the bulb diameter produced by water is larger than that produced by other lubricants. Figure 8(b) shows the worn surface of a PEEK ball subjected to 10 wt% PVA as a lubricant. The wear diameter is reduced, and the wear debris cannot be easily observed in comparison to water lubrication. Figure 8(c) shows the worn surface of a PEEK ball subjected to 15 wt% PEG as a lubricant. The wear area of the PEEK sphere is significantly lesser than that of water and identical to that of PVA; however, the wear debris on the surface can be easily observed. Figure 8(d) shows the worn surface of a PEEK subjected to PVA/PEG gel (10 wt %/15 wt%) as a lubricant. The wear area produced by this gel was less than that of the other substances. In addition, the wear debris were small and barely visible. The corresponding disks do not appear to be worn out. Therefore, the wear spots on the surface of the PEEK sphere may be caused by indentation. This is attributed to the combined positive effect of the two components of the gel, which simultaneously address different aspects of lubrication.

3.9. Schematic and Biological Analysis. The COF is calculated by applying positive pressure on the PEEK ball in such a way that the gel remains in position between the ball and the disk [54]. The reciprocating motion records the pressure that needs to be applied. The white gelatinous substance, which is formed because of the combined properties of PVA and PEG, is equivalent to PVA wrapped around PEG. Figure 9(a) shows the wear rates and volumes of four lubricants, namely water, 10 wt% PVA, 15 wt% PEG, and the gel under positive pressure. The wear volume and wear rate of water as a lubricant are relatively large, while the wear volume and wear rate of the gel are less than those of the other lubricants, indicating that the prepared gel has high wear resistance. Figure 9(b) shows the absorbance value (OD value), which was measured at 540 nm by an enzyme-linked immunoassay. This value was expressed in cell proliferation rates with respect to the control group. It is evident that the cell growth

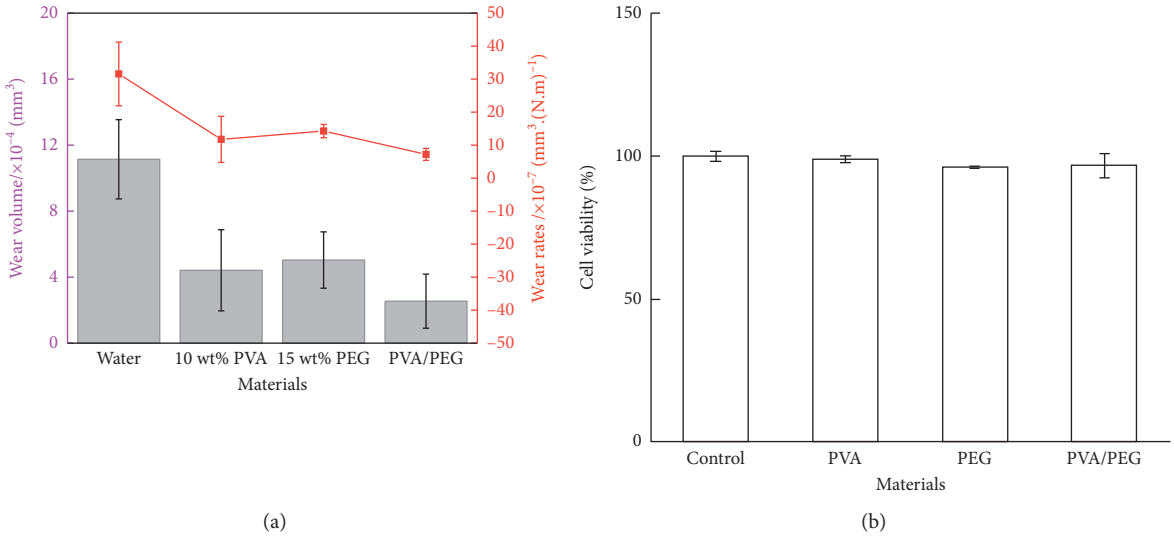

(a) (b)

Figure 9: (a) Wear volume and rates for different lubricants and (b) cell viability by MTT.

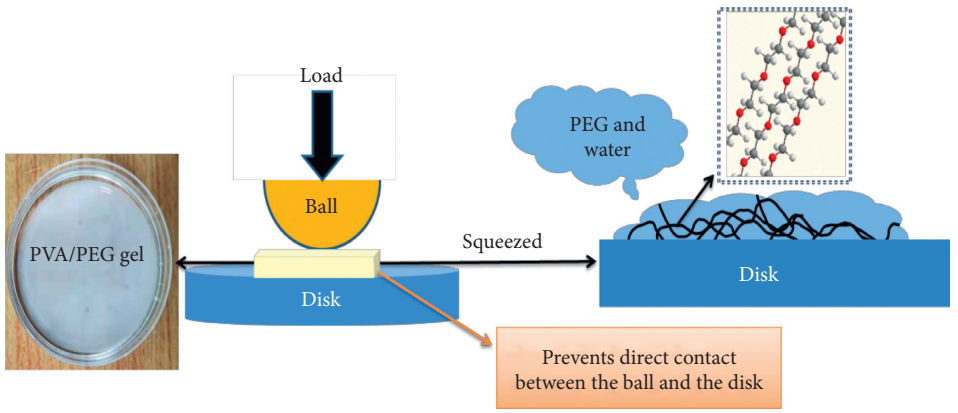

Figure 10: Schematic of the lubrication mechanism.

was almost uninhibited. The cell proliferation rates of the PVA, PEG, and PVA/PEG gels were similar to that of the control group, thereby proving the biocompatibility of the PVA/PEG gel.

3.10. Lubrication Mechanism Analysis. PVA is a polymer with a large number of hydroxyl groups attached to the main chain. Water molecules are more likely to be trapped in the voids of the PVA chains of partially hydrolyzed PVA, thereby triggering the formation of water-rich cage-like structures that rapidly exchange bound or free water molecules [55]. The lubricating fluid is mediated by the formation of a normal fluid film [56]. This structure prevents direct contact between the two substances [57], resulting in reduced wear. In aqueous media, PEG chains form a "brush" structure at the interface after hydration, which reduces the friction between the surfaces. Several studies have analyzed the gels formed by cross-linking PVA and PEG; however, only a few studies have investigated their lubrication properties [46, 58, 59]. The PVA/PEG gel was developed in this study by adding PVA to the PEG solution. Thus, the PVA/PEG gel comprised PEG chains and water, as shown in Figure 10 illustrating a schematic of the lubrication effect. In the friction experiment, the PEG and water molecules in the PVA/PEG gel are squeezed out, filling the surface of the disk and reducing the COF. Meanwhile, the PVA/PEG gel acts as a membrane that separates the two substances from direct contact, which ultimately leads to reduced wear.

4. Conclusions

A PVA/PEG gel was developed in this study by adding polyvinyl alcohol to a polyethylene glycol solution. Solutions with varying concentrations were prepared, followed by methodological stirring to produce an appropriate gel. Friction tests, FT-IR spectroscopy, and an immunoassay were used to analyze the reduction in the COF, specific reactions between different components, and the gel's biological properties, respectively. The lubrication and wear resistance of PVA/PEG gels were established by conducting the friction and wear test, which proved that the gel had a better lubrication effect than that of the PVA and PEG materials at a certain pressure. The gel formed an isolation

film because of the presence of PVA, which prevented the two substances from coming in direct contact, thereby reducing wear. In contrast, the presence of PEG improved its lubrication performance. The molecular properties of the gel were analyzed using the FT-IR, XRD, XPS, and TGA techniques. In addition, biological experiments demonstrated that the gel was highly biocompatible, thereby demonstrating its potential for application in artificial joints.

Data Availability

All the data are included in the manuscript.

Conflicts of Interest

The authors declare that they have no conflicts of interest or personal relationships that could have appeared to influence the work reported in this paper.

Authors' Contributions

Feng Hu, Shoujing Zhang, and Hailin Lu developed the initial concept. Feng Hu and Hailin Lu wrote the initial paper. Jianhui Li and Leifeng Lv provided assistance for data acquisition and data analysis. All authors discussed the results and commented on the manuscript. Feng Hu and Shoujing Zhang contributed equally to this work and should be considered co-first authors.

Acknowledgments

This work was supported by the National Key Research and Development Program of China (2019YFB1707205) and the Xi'an Key Laboratory of Modern Intelligent Textile Equipment (no. 2019220614SYS021CG043).

References

[1] B. Bai, J. Zhou, and M. Yin, "A comprehensive review of polyacrylamide polymer gels for conformance control," *Petroleum Exploration and Development*, vol. 42, no. 4, pp. 525–532, 2015.

[2] L. Chen, T. Ye, Y. Liu et al., "Gel network incorporation into single-crystals: effects of gel structures and crystal-gel interaction," *CrystEngComm*, vol. 16, no. 30, pp. 6901–6906, 2014.

[3] I. E. Hamilton and I. T. Norton, "Modification to the lubrication properties of xanthan gum fluid gels as a result of sunflower oil and triglyceride stabilised water in oil emulsion addition," *Food Hydrocolloids*, vol. 55, pp. 220–227, 2016.

[4] V. Urbonaite, H. H. J. de Jongh, E. van der Linden, and L. Pouvreau, "Permeability of gels is set by the impulse applied on the gel," *Food Hydrocolloids*, vol. 50, pp. 7–15, 2015.

[5] J. Erdmann, "Replacing worn out joints: new materials and designs come to artificial hips and knees," *Chemistry & Biology*, vol. 18, no. 7, pp. 817-818, 2011.

[6] A. Escobar, J. Quintana, M. González et al., "Pms64 differences in quality of life according to the replaced joint," *Value in Health*, vol. 11, no. 6, p. A557, 2008.

[7] M. Tayebi, D. Bizari, and Z. Hassanzade, "Investigation of mechanical properties and biocorrosion behavior of in situ and ex situ Mg composite for orthopedic implants," *Materials Science & Engineering C-Materials for Biological Applications*, vol. 2020, p. 113, Article ID 110974, 2020.

[8] H. F. Wang, D. W. Zuo, S. R. Liu, J. F. Pu, and W. W. Song, "Wear resistance analysis of a lightweight aluminum alloy sheet friction stir joint area," *Strength of Materials*, vol. 52, no. 4, pp. 565–572, 2020.

[9] J. Wang, D. Zhou, Y. Lu et al., "Effects of laser shock peening on the mechanical behaviors and microstructure of friction stir processed 2a14 aluminum alloy," *Journal of Materials Engineering and Performance*, vol. 30, pp. 239–247, 2020.

[10] X. Lu, Q. Meng, J. Wang, and Z. Jin, "Transient viscoelastic lubrication analyses of UHMWPE hip replacements," *Tribology International*, vol. 128, pp. 271–278, 2018.

[11] T. Murakami, N. Sakai, T. Yamaguchi et al., "Evaluation of a superior lubrication mechanism with biphasic hydrogels for artificial cartilage," *Tribology International*, vol. 89, pp. 19–26, 2015.

[12] J. Zhu, F. Xie, and R. S. Dwyer-Joyce, "PEEK composites as self-lubricating bush materials for articulating revolute pin joints," *Polymers*, vol. 12, no. 3, 2020.

[13] D. Baykal, R. S. Siskey, R. J. Underwood, A. Briscoe, and S. M. Kurtz, "The biotribology of PEEK-on-HXLPE bearings is comparable to traditional bearings on a multidirectional pin-on-disk tester," *Clinical Orthopaedics and Related Research*, vol. 474, no. 11, pp. 2384–2393, 2016.

[14] R. Sedlacek and J. Rosenkrancova, "The wear resistance testing of biomaterials used for implants," in *Bioceramics*, M. A. Barbosa, F. J. Monteiro, R. Correia, and B. Leon, Eds., vol. 16pp. 703–706, 2004.

[15] M. Regis, A. Lanzutti, P. Bracco, and L. Fedrizzi, "Wear behavior of medical grade PEEK and CFR PEEK under dry and bovine serum conditions," *Wear*, vol. 408-409, pp. 86–95, 2018.

[16] H. Xu, D. Zhang, K. Chen, and T. Zhang, "Taper fretting behavior of PEEK artificial hip joint," *Tribology International*, vol. 137, pp. 30–38, 2019.

[17] J. Zhu, L. Ma, and R. Dwyer-Joyce, "Friction and wear behaviours of self-lubricating peek composites for articulating pin joints," *Tribology International*, vol. 149, Article ID 105741, 2020.

[18] H. Xu, K. Chen, D. Zhang, and X. Yang, "Torsional friction behavior of the contact interface between the materials of an artificial knee joint replacement," *Journal of Biomaterials Science, Polymer Edition*, vol. 29, no. 5, pp. 562–581, 2018.

[19] K. Chen, D. Zhang, X. Yang, X. Zhang, Q. Wang, and J. Qi, "Swing friction behavior of the contact interface between CoCrMo and UHMWPE under dynamic loading," *Journal of Materials Engineering and Performance*, vol. 25, no. 12, pp. 5400–5410, 2016.

[20] R. Crockett, M. Roba, M. Naka et al., "Friction, lubrication, and polymer transfer between UHMWPE and CoCrMo hip-implant materials: a fluorescence microscopy study," *Journal of Biomedical Materials Research Part A*, vol. 89A, no. 4, pp. 1011–1018, 2009.

[21] M. Wu, K. Chen, L. Xu, J. Qi, Y. Luo, and D. Zhang, "Swing-torsion composite friction behavior of CoCrMo/UHMWPE contact interface of artificial knee joint prosthesis implantation materials," *Materials Research Express*, vol. 6, no. 5, 2019.

[22] Y. Kanca, P. Milner, D. Dini, and A. A. Amis, "Tribological properties of PVA/PVP blend hydrogels against articular cartilage," *Journal of the Mechanical Behavior of Biomedical Materials*, vol. 78, pp. 36–45, 2018.

[23] O. K. Muratoglu, K. Wannomae, S. Christensen, H. E. Rubash, and W. H. Harris, "Ex vivo wear of conventional and cross-

linked polyethylene acetabular liners," *Clinical Orthopaedics and Related Research*, vol. 438, pp. 158–164, 2005.

[24] H. Lu, S. Ren, X. Li et al., "Poly(ethylene glycol)/chitosan/sodium glycerophosphate gel replaced the joint capsule with slow-release lubricant after joint surgery," *Journal of Biomaterials Science, Polymer Edition*, vol. 29, no. 11, pp. 1331–1343, 2018.

[25] H. Lu, L. Chen, Q. Liu, Y. Li, and L. Gao, "Tribological properties of biocompatible molybdenum selenide nanoparticles as water lubrication additives for ultra-high molecular weight polyethylene/304 stainless steel contact," *Materials Chemistry and Physics*, vol. 272, Article ID 125053, 2021.

[26] Q. Zhang, G. Han, C. Lu et al., "Facile preparation of mechanical reinforced and biocompatible silk gels," *Fibers and Polymers*, vol. 20, no. 4, pp. 675–682, 2019.

[27] S. Z. Bonyadi, M. M. Hasan, J. Kim, S. Mahmood, K. D. Schulze, and A. C. Dunn, "Review: friction and lubrication with high water content crosslinked hydrogels," *Tribology Letters*, vol. 68, no. 4, 2020.

[28] W. Liu, R. Simic, Y. Liu, and N. D. Spencer, "Effect of contact geometry on the friction of acrylamide hydrogels with different surface structures," *Friction*, 2020.

[29] L. Wang, T. Hou, Y. Li, H. Lu, and L. Gao, "Lubrication performances of carbon-doped MoSe2 nanoparticles and their biocompatibility characterization in vitro," *Frontiers in Chemistry*, vol. 8, Article ID 580151, 2021.

[30] F. Li, Z. Lu, H. Qian et al., "Preparation and size determination of soluble cross-linked macromolecule of polyurethane," *Macromolecules*, vol. 37, no. 3, pp. 764–768, 2004.

[31] D. Winter and C. D. Eisenbach, "Synthesis and characterization of novel aryl-ethynylene polymers of tuned rigidity/flexibility," *Journal of Polymer Science Part A: Polymer Chemistry*, vol. 42, no. 8, pp. 1919–1933, 2004.

[32] J. K. Katta, M. Marcolongo, A. Lowman, and K. A. Mansmann, "Friction and wear behavior of poly(vinyl alcohol)/poly(vinyl pyrrolidone) hydrogels for articular cartilage replacement," *Journal of Biomedical Materials Research Part A*, vol. 83A, no. 2, pp. 471–479, 2007.

[33] X. Li, H. Qin, X. Zhang, and Z. Guo, "Triple-network hydrogels with high strength, low friction and self-healing by chemical-physical crosslinking," *Journal of Colloid and Interface Science*, vol. 556, pp. 549–556, 2019.

[34] F. Li, G. Zhang, A. Wang, and F. Guo, "The effects of surface mechanical deformation and bovine serum albumin on the tribological properties of polyvinyl alcohol hydrogel as an artificial cartilage," *Advances in Materials Science and Engineering*, vol. 2017, Article ID 4502904, , 2017.

[35] H.-Y. Chou and H.-C. Tsai, "Development of hydrogels with thermal-healing properties using a network of polyvinyl alcohol and boron nitride composites," *Materials Science and Engineering: C*, vol. 118, Article ID 111364, 2021.

[36] Q. Zhou, T. Li, C. Li, M. Ye, Y. Lu, and Y. Duan, "Biocompatibility of implantable electrodes coated with PVA films in the brain of rats: a histological evaluation," *Journal of Wuhan University of Technology-Materials Science Edition*, vol. 24, no. 3, pp. 393–396, 2009.

[37] P. Kuchaiyaphum, G. Rifai, W. Yuuki, and T. Yamauchi, "Hyaluronic acid-poly(vinyl alcohol) composite cryo-gel for biofunctional material application," *Polymers for Advanced Technologies*, vol. 30, no. 1, pp. 94–100, 2019.

[38] R. Atchudan, T. N. J. I. Edison, M. G. Sethuraman, and Y. R. Lee, "Efficient synthesis of highly fluorescent nitrogen-doped carbon dots for cell imaging using unripe fruit extract of Prunus mume," *Applied Surface Science*, vol. 384, pp. 432–441, 2016.

[39] Z. Feng, F. Hu, L. Lv, L. Gao, and H. Lu, "Preparation of ultra-high mechanical strength wear-resistant carbon fiber textiles with a PVA/PEG coating," *RSC Advances*, vol. 11, no. 41, pp. 25530–25541, 2021.

[40] X. Gao, Y. Zhou, G. Ma et al., "A water-soluble photo-crosslinkable chitosan derivative prepared by Michael-addition reaction as a precursor for injectable hydrogel," *Carbohydrate Polymers*, vol. 79, no. 3, pp. 507–512, 2010.

[41] J. Cao, Y. Meng, X. Zhao, and L. Ye, "Dual-anchoring intercalation structure and enhanced bioactivity of poly(vinyl alcohol)/graphene oxide-hydroxyapatite nanocomposite hydrogels as artificial cartilage replacement," *Industrial & Engineering Chemistry Research*, vol. 59, no. 46, pp. 20359–20370, 2020.

[42] X. Jing, H. Li, H.-Y. Mi et al., "Highly transparent, stretchable, and rapid self-healing polyvinyl alcohol/cellulose nanofibril hydrogel sensors for sensitive pressure sensing and human motion detection," *Sensors and Actuators B: Chemical*, vol. 295, pp. 159–167, 2019.

[43] Q. Ding, X. Xu, Y. Yue et al., "Nanocellulose-mediated electroconductive self-healing hydrogels with high strength, plasticity, viscoelasticity, stretchability, and biocompatibility toward multifunctional applications," *ACS Applied Materials & Interfaces*, vol. 10, no. 33, pp. 27987–28002, 2018.

[44] S.-Y. Lin, W.-T. Cheng, Y.-S. Wei, and H.-L. Lin, "DSC-FTIR microspectroscopy used to investigate the heat-induced intramolecular cyclic anhydride formation between Eudragit E and PVA copolymer," *Polymer Journal*, vol. 43, no. 6, pp. 577–580, 2011.

[45] H. S. Mansur, R. L. Oréfice, and A. A. P. Mansur, "Characterization of poly(vinyl alcohol)/poly(ethylene glycol) hydrogels and PVA-derived hybrids by small-angle X-ray scattering and FTIR spectroscopy," *Polymer*, vol. 45, no. 21, pp. 7193–7202, 2004.

[46] F. H. Falqi, O. A. Bin-Dahman, M. Hussain, and M. A. Al-Harthi, "Preparation of miscible PVA/PEG blends and effect of graphene concentration on thermal, crystallization, morphological, and mechanical properties of PVA/PEG (10wt%) blend," *International Journal of Polymer Science*, vol. 2018, Article ID 8527693, 10 pages, 2018.

[47] M. A. Hussein, B. M. Abu-Zied, and A. M. Asiri, "Preparation, characterization, and electrical properties of ZSM-5/PEG composite particles," *Polymer Composites*, vol. 35, no. 6, pp. 1160–1168, 2014.

[48] G. Fortunato, A. G. Guex, A. M. Popa, R. M. Rossi, and R. Hufenus, "Molecular weight driven structure formation of PEG based e-spun polymer blend fibres," *Polymer*, vol. 55, no. 14, pp. 3139–3148, 2014.

[49] Y. Tian, M. Chen, S. Xue et al., "Template-determined microstructure and electrochemical performances of Li-rich layered metal oxide cathode," *Journal of Power Sources*, vol. 401, pp. 343–353, 2018.

[50] S. Lee and N. D. Spencer, "Aqueous lubrication of polymers: influence of surface modification," *Tribology International*, vol. 38, no. 11-12, pp. 922–930, 2005.

[51] G. Dong, Y. Liu, M. Jing, F. Wang, and H. Liu, "Effect of elastohydrodynamic lubrication on the dynamic analysis of ball bearing," *Proceedings of the Institution of Mechanical Engineers - Part K: Journal of Multi-Body Dynamics*, vol. 230, no. 2, pp. 134–146, 2016.

[52] Z. A. Khan, M. Hadfield, S. Tobe, and Y. Wang, "Residual stress variations during rolling contact fatigue of refrigerant

lubricated silicon nitride bearing elements," *Ceramics International*, vol. 32, no. 7, pp. 751–754, 2006.

[53] Y. S. Pan, D. S. Xiong, and X. L. Chen, "Friction behavior of poly(vinyl alcohol) gel against stainless steel ball in different lubricant media," *Journal of Tribology - Transactions of the ASME*, vol. 130, no. 3, p. 5, 2008.

[54] I. Clavería, S. Gimeno, and I Miguel, "Tribological performance of nylon composites with nanoadditives for self-lubrication purposes," *Polymers*, vol. 12, no. 10, 2020.

[55] Q. Fang, F. Ye, and X. Yang, "Influence of hydrolysis of polyvinyl alcohol on its lubrication for styrene-ethylene-butylene-styrene block copolymer," *Tribology International*, vol. 134, pp. 408–416, 2019.

[56] R. Y. Ma, D. S. Xiong, F. Miao, J. F. Zhang, and Y. Peng, "Friction properties of novel PVP/PVA blend hydrogels as artificial cartilage," *Journal of Biomedical Materials Research Part A*, vol. 93A, no. 3, pp. 1016–1019, 2010.

[57] P. C. Nalam, J. N. Clasohm, A. Mashaghi, and N. D. Spencer, "Macrotribological studies of poly(L-lysine)-graft-poly(ethylene glycol) in aqueous glycerol mixtures," *Tribology Letters*, vol. 37, no. 3, pp. 541–552, 2010.

[58] C. Zhao, X. Lu, Q. Hu, S. Liu, and S. Guan, "PVA/PEG hybrid hydrogels prepared by freeze-thawing and high energy electron beam irradiation," *Chemical Research in Chinese Universities*, vol. 33, no. 6, pp. 995–999, 2017.

[59] R. Ahmed, A. Ibrahim, and E. El-Said, "Enhancing the optical properties of polyvinyl alcohol by blending it with polyethylene glycol," *Acta Physica Polonica A*, vol. 137, no. 3, pp. 317–323, 2020.